

Image charge effect on the light emission of rutile TiO_2(110) induced by a scanning tunneling microscope

Chaoyu Guo(郭钞宇), Xiangzhi Meng(孟祥志), Qin Wang(王钦), Ying Jiang(江颖)

Citation: Chin. Phys. B . 2018, 27(7): 077301. **doi:** 10.1088/1674-1056/27/7/077301

Journal homepage: http://cpb.iphy.ac.cn; http://iopscience.iop.org/cpb

What follows is a list of articles you may be interested in

Enhanced photoresponse performance in Ga/Ga_2O_3 nanocomposite solar-blind ultraviolet photodetectors

Shu-Juan Cui(崔书娟), Zeng-Xia Mei(梅增霞), Yao-Nan Hou(侯尧楠), Quan-Sheng Chen(陈全胜), Hui-Li Liang(梁会力), Yong-Hui Zhang(张永晖), Wen-Xing Huo(霍文星), Xiao-Long Du(杜小龙)

Chin. Phys. B . 2018, 27(6): 067301. **doi:** 10.1088/1674-1056/27/6/067301

Resonant surface plasmons of a metal nanosphere treated as propagating surface plasmons

Yu-Rui Fang(方蔚瑞), Xiao-Rui Tian(田小锐)

Chin. Phys. B . 2018, 27(6): 067302. **doi:** 10.1088/1674-1056/27/6/067302

Gap plasmon-enhanced photoluminescence of monolayer MoS_2 in hybrid nanostructure

Le Yu(余乐), Di Liu(刘頔), Xiao-Zhuo Qi(祁晓卓), Xiao Xiong(熊霄), Lan-Tian Feng(冯兰天), Ming Li(李明), Guo-Ping Guo(郭国平), Guang-Can Guo(郭光灿), Xi-Feng Ren(任希锋)

Chin. Phys. B . 2018, 27(4): 047302. **doi:** 10.1088/1674-1056/27/4/047302

Highly stable two-dimensional graphene oxide: Electronic properties of its periodic structure and optical properties of its nanostructures

Qin Zhang(张琴), Hong Zhang(张红), Xin-Lu Cheng(程新路)

Chin. Phys. B . 2018, 27(2): 027301. **doi:** 10.1088/1674-1056/27/2/027301

Elastic scattering of surface states on three-dimensional topological insulators

Wang Jing, Zhu Bang-Fen

Chin. Phys. B . 2013, 22(6): 067301. **doi:** 10.1088/1674-1056/22/6/067301

RAPID COMMUNICATION

Image charge effect on the light emission of rutile TiO_2(110) induced by a scanning tunneling microscope*

Chaoyu Guo(郭钞宇)[1], Xiangzhi Meng(孟祥志)[1], Qin Wang(王钦)[1], and Ying Jiang(江颖)[1,2,3,†]

[1] International Center for Quantum Materials, School of Physics, Peking University, Beijing 100871, China
[2] Collaborative Innovation Center of Quantum Matter, Beijing 100871, China
[3] CAS Center for Excellence in Topological Quantum Computation, University of Chinese Academy of Sciences, Beijing 100049, China

(Received 25 May 2018; published online 25 June 2018)

The plasmon-enhanced light emission of rutile TiO_2(110) surface has been investigated by a low-temperature scanning tunneling microscope (STM). We found that the photon emission arises from the inelastic electron tunneling between the STM tip and the conduction band or defect states of TiO_2(110). In contrast to the Au(111) surface, the maximum photon energy as a function of the bias voltage clearly deviates from the linear scaling behavior, suggesting the non-negligible effect of the STM tip on the band structure of TiO_2. By performing differential conductance (dI/dV) measurements, it was revealed that such a deviation is not related to the tip-induced band bending, but is attributed to the image charge effect of the metal tip, which significantly shifts the band edges of the TiO_2(110) towards the Femi level (E_F) during the tunneling process. This work not only sheds new lights onto the understanding of plasmon-enhanced light emission of semiconductor surfaces, but also opens up a new avenue for engineering the plasmon-mediated interfacial charge transfer in molecular and semiconducting materials.

Keywords: scanning tunneling microscopy, light emission, TiO_2, plasmon

PACS: 73.20.–r, 73.20.Mf, 74.55.+v, 78.60.Fi **DOI:** 10.1088/1674-1056/27/7/077301

1. Introduction

The light emission induced by the tunneling current of scanning tunneling microscope (STM) has received increasing attention recently, since it provides the unprecedented possibility of studying the electron-photon conversion at the atomic scale,[1–6] which is critical for understanding and controlling the properties of future nanoscale optoelectronic devices. Inelastic electron tunneling (IET) process can excite the localized surface plasmon (LSP) modes confined within the cavity between STM tip and the metal substrate. Those LSP modes decay into propagating photons in free space, which are detectable by far-field optical setups (Figs. 1(a) and 1(b)). The high spatial resolution of STM-induced light emission arises from the highly local charge injection and excitation through the tunneling current. The STM-induced light emission was first reported in 1989 by Gimzewski *et al.*[1] Ever since, the light emission of various systems has been extensively investigated by STM, focusing on metals surfaces,[7,8] adsorbed molecules,[9–11] quantum wells,[12] artificial nanostructures,[13,14] and so on. However, the light-emission experiments on semiconductor surfaces are very rare and our understanding of the microscopic mechanism is still far from complete.

There are several difficulties for studying the plasmon-enhanced light emission on semiconducting materials by STM. First, the free-carrier density in semiconductors is much less than that in metals, leading to a much weaker plasmonic field.[15] Therefore, the plasmon enhancement of the tip-surface cavity is not as efficient as metal surfaces and the photon emission should be rather weak on semiconducting surfaces. Second, the band structure of semiconductors is more complicated than that of metals. The dopants and defects often induce prominent in-gap states,[16–18] which greatly modulate the inelastic electronic transition and thus the light emission process. Third, the STM tip can induce significant changes in the electronic structure of semiconductors, such as tip-induced band bending[19–21] and image charge effect.[22–25] In this work, we choose to investigate the rutile TiO_2(110), which is one of the most widely studied materials in photoconversion and photocatalysis. We are able to obtain high-quality spectroscopy of light emission using our homemade optical STM and the effect of STM tip on the light emission is unambiguously revealed.

2. Experimental details

The experiments were performed with a homemade ultra-high vacuum (UHV) STM system, with a base pressure better than 2×10^{-10} mbar. A rutile TiO_2(110) single crystal (MaT-

*Project supported by the National Key R&D Program of China (Grant Nos. 2016YFA0300901 and 2017YFA0205003), the National Natural Science Foundation of China (Grant Nos. 11634001 and 21725302), and the Key Research Program of the Chinese Academy of Sciences (Grant No. XDPB08-1).

†Corresponding author. E-mail: yjiang@pku.edu.cn

© 2018 Chinese Physical Society and IOP Publishing Ltd

ech) was cleaned with cycles of sputtering by Neon ions and annealing at about 1000 K. In order to increase the conductivity at low temperature, the TiO_2 sample was prepared with a high concentration of surface and subsurface defects. After the surface preparation, the sample was transferred immediately to the cryogenic STM stage to avoid the contamination of the TiO_2(110) surface.

The STM characterization and light emission experiments of the TiO_2(110) surface were performed with electrochemically etched silver tips. The scanning tunneling spectroscopy (STS) was acquired using lock-in detection of the tunneling current by adding a 13 mV_{rms} modulation at 287 Hz to the sample bias at 5 K. Bias voltage refers to the sample voltage with respect to the tip.

Photons emitted from the tunneling junction were collected by a UHV compatible aspheric lens (Edmund Optics, EFL = 20 mm, N.A. = 0.38), which was fixed to a high-precision nanopositioner (Attocube) and then guided through a mirror system into a grating spectrometer coupled to a liquid-nitrogen-cooled charge-coupled device (CCD) (Princeton Instrument, SP2300). All light emission experiments were carried out at a sample temperature of 77 K. All the emission spectra were acquired at constant-current mode.

3. Results and discussion

Owing to their characteristic dielectric function, noble metals support strong surface plasmon oscillations in the energy range corresponding to the visible lights.[26,27] The shape and intensity maxima of the light emission spectrum correspond to particular modes of plasmon resonance, determined by both the tip and the sample. For Au(111), it emits red lights when a bias of a few volts is applied. Figure 1(c) shows a series of emission spectra of the Au(111) surface at 77 K with varying sample bias from 1.5 to 3.5 V. The broad peak around 1.96 eV (630 nm) corresponds to the LSP resonance mode. The cut-off wavelength (maximum photon energy, E_{max}) of the spectral distribution (denoted by the arrows in Fig. 1(c)) exhibits a continuous blueshift when increasing the sample bias. In Fig. 1(d), we plot E_{max} as a function of the bias voltage, showing a perfect linear relation, accompanied with a level-off when the bias voltage is larger than 2.4 V. In the linear region, the maximum photon energies are identical to eV, consistent with the picture of IET-induced light emission (Fig. 1(b)). The maximum photon energies beyond the bias of 2.4 V are limited by the energy range of the LSP mode.

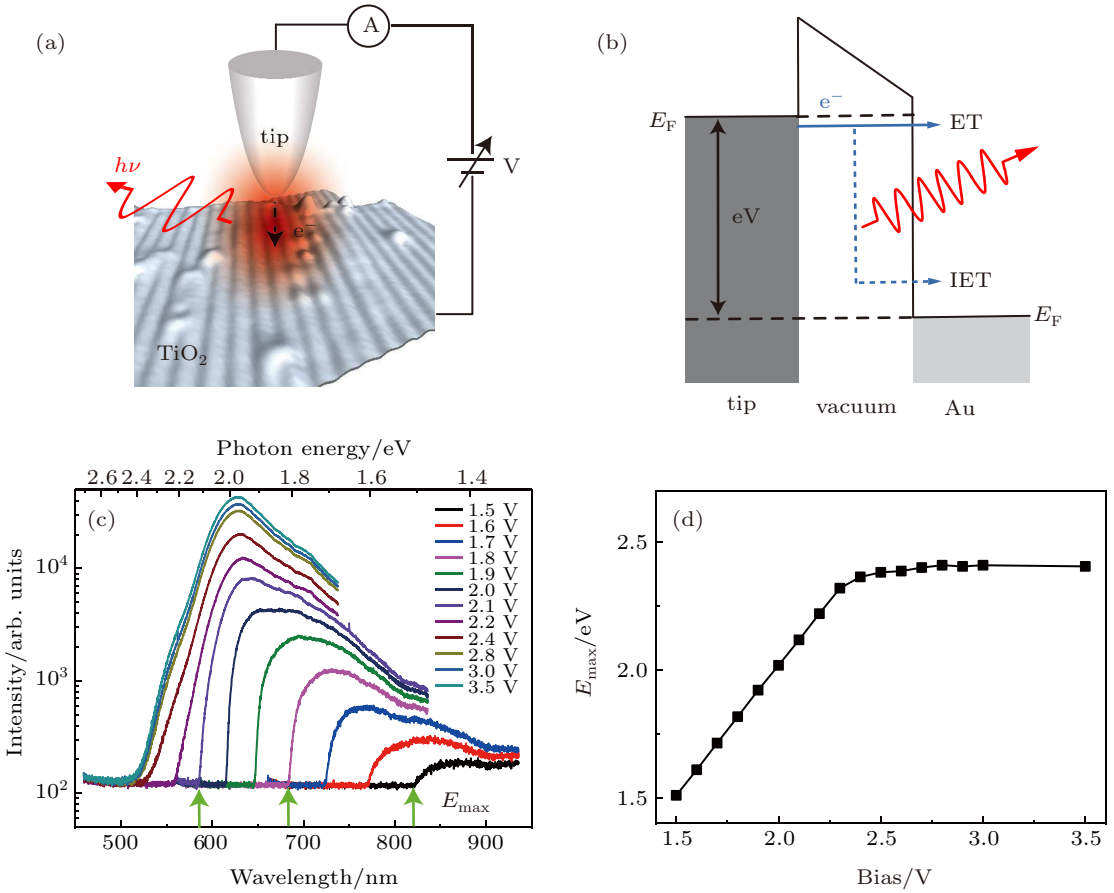


Fig. 1. (color online) (a) Schematic of plasmon-enhanced light emission in the STM junction. (b) Energy diagram illustrating the mechanism for light emission of Au(111) sample. Elastic (ET) and inelastic tunneling (IET) processes are indicated by solid and dashed arrows, respectively. (c) Light emission spectra recorded on the bare Au(111) surface (constant-current mode, $I = 2$ nA, $V = 1.5$ V–3.5 V). The green arrows indicate the cut-off wavelengths (maximum photon energy, E_{max}) of the light emission spectra. (d) The maximum photon energy (E_{max}) as a function of bias voltage.

For semiconductor, such as TiO_2, the mechanism of STM-induced light emission is similar with that of noble metal samples (Figs. 2(a) and 2(b)). However, the maximum photon energy E_{max} is smaller than eV due to the existence of the bandgap. For $V > 0$, the light emission is induced by the inelastic electronic transition between the tip and the conduction band, and $E_{max} = eV - E_{CB}$, where E_{CB} is the position of conduction band edge with respect to the Fermi level (E_F) of TiO_2 (Fig. 2(a)). For $V < 0$, the photons are generated by the electrons inelastically tunneling from the valence band to the tip and $E_{max} = e|V| + E_{VB}$ (Fig. 2(b)). It should be noted that surface/subsurface defects on TiO_2 such as oxygen vacancies and Ti interstitials may lead to prominent in-gap states (E_d) below the E_F.[28,29] In this case, the maximum photon energy $E_{max} = e|V| + E_d^{upper}$, where E_d^{upper} is the upper energy bound of defect states with respect to E_F.

Figure 2(c) shows a series of emission spectra taken at a defective area of TiO_2(110) with varying bias voltage from 3 V to 4 V, where the cut-off wavelengths are highlighted by arrows. The relationship between the maximum photon energy (E_{max}) and the sample bias is shown in Fig. 2(d), indicating a clear deviation from the linear behavior. Similar to the case of Au(111), E_{max} tends to level off at large biases (see the dashed lines). We then calculated E_{CB} and E_d^{upper} by subtracting E_{max} from the energy of tunneling electrons (eV) before the level-off region. The results are shown in Fig. 2(e). It is interesting that both the band edges experience a noticeable shift towards E_F when decreasing the bias voltage. It is worth noting that constant current mode was used during the light-emission measurements, so the tip is actually approaching the sample when the bias voltage is decreased.

In order to understand the origin of the band edge shift, we carried out systematic dI/dV measurements for TiO_2 surface. A series of STS spectra were taken at the defective area with different tip heights (Fig. 3(a)), showing a distinct bandgap narrowing as the tip height decreases. We plot the energy of conduction and valence band edges as a function of the tip height in Fig. 3(b). It is striking that both edges shift towards E_F when the tip is advanced to the surface, which is very similar to the band edge shift observed in Fig. 2(e). In addition, we found the defect states (E_d) also show considerable upward shift as decreasing the tip-surface separation (Figs. 3(c) and 3(d)), suggesting that the apparent shift of the valence band edge in Figs. 3(a) and 3(b) should correspond to the shift of upper energy bound of the defect states (E_d^{upper}).

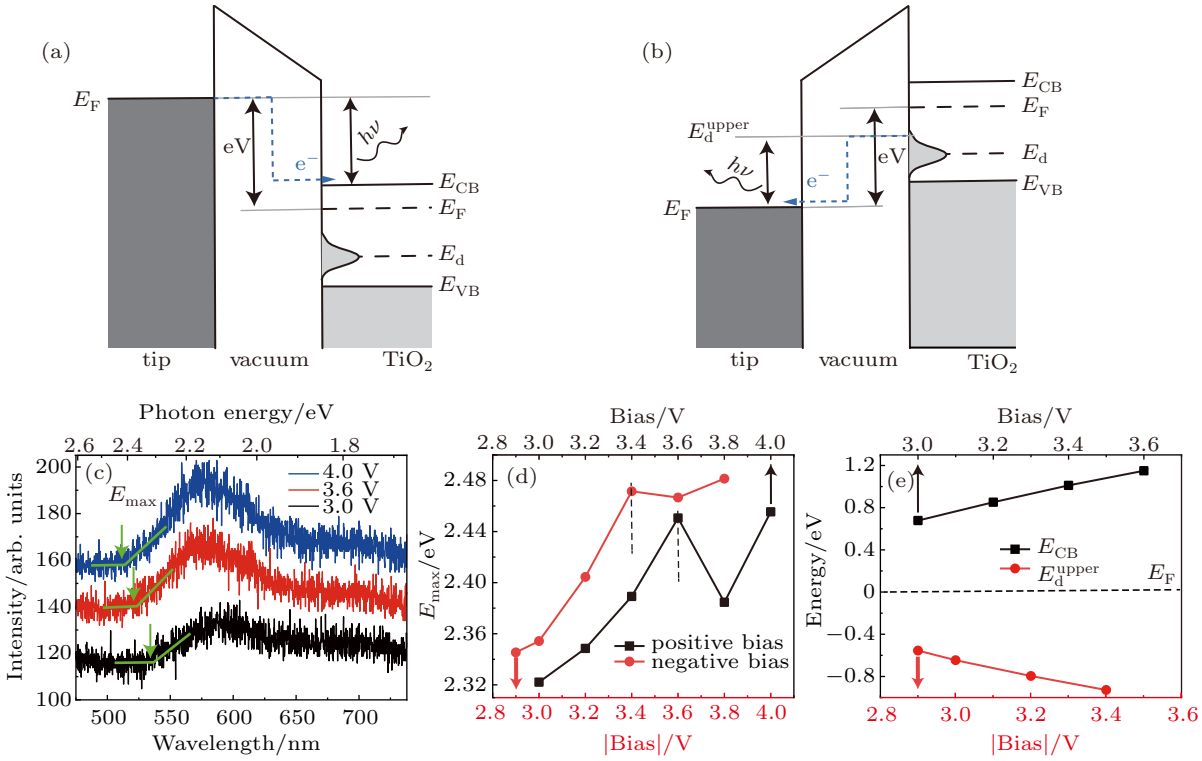


Fig. 2. (color online) (a), (b) Energy diagrams illustrating the mechanism for light emission of TiO_2(110) sample at positive and negative biases, respectively. The conduction band minimum (E_{CB}), valence band maximum (E_{VB}), Fermi level (E_F), defect state (E_d) are indicated. The upper energy bound of defect state is denoted by E_d^{upper}. The double-headed arrows denote the sample bias (V) and the emitted photon energy ($h\nu$). The blue dashed line represents the inelastic tunneling processes. (c) Light emission spectra recorded at the defective TiO_2(110) surface (constant-current mode, $I = 3$ nA, $V = 3.0$ V–4.0 V). The spectra are offset for clarity. The green arrows indicate the cut-off wavelengths (maximum photon energy, E_{max}). (d) The maximum photon energy (E_{max}) measured at positive (black) and negative (red) sample biases. The dashed lines mark the level-off bias voltage. (e) The energies of band edges (E_{CB} and E_d^{upper}) deduced from light emission spectra at positive (black) and negative (red) sample biases, respectively.

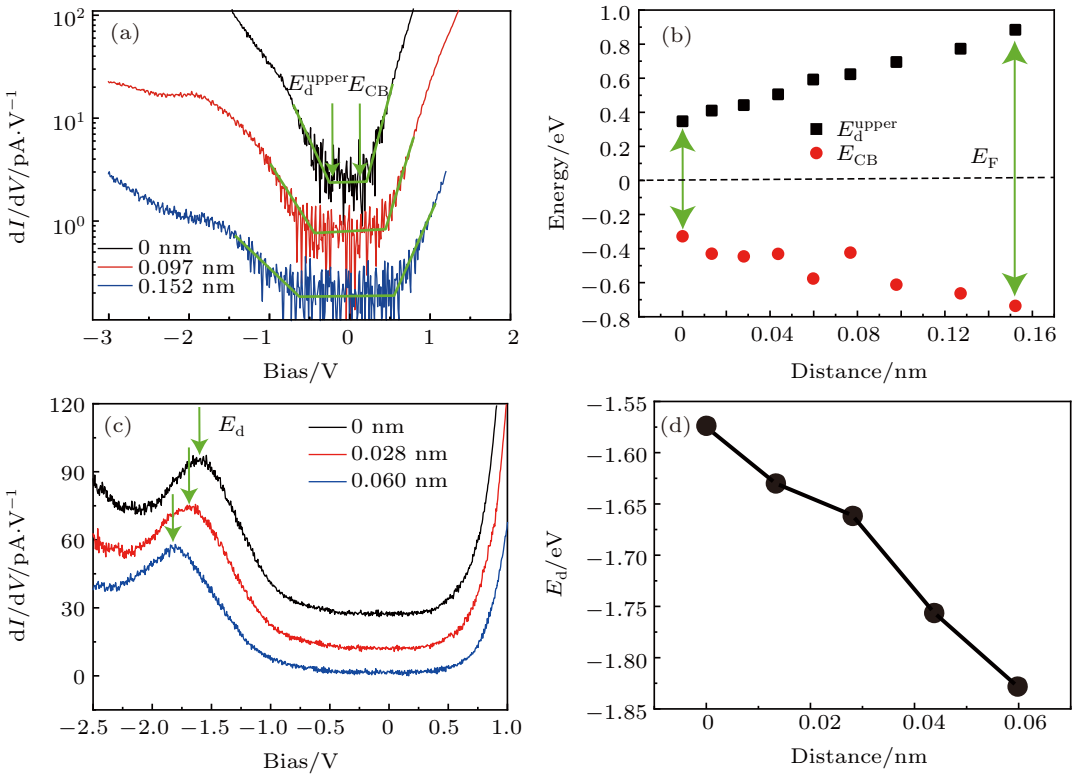


Fig. 3. (color online) (a) $\mathrm{d}I/\mathrm{d}V$ spectra taken at the defective TiO_2(110) surface with different tip-sample distance in Logarithmic scale. The tip heights refer to the set point of 1.7 V/0.8 nA (0 nm). The spectrum taken at 0.097 nm and 0 nm were offset by 1.2 pA/V and 3.6 pA/V for clarity, respectively. The band edges are denoted by green arrows. (b) Band edge energies derived from the $\mathrm{d}I/\mathrm{d}V$ spectra at different tip-sample distances. The green double-headed arrows show the energy gap between the conduction band and defect states. (c) $\mathrm{d}I/\mathrm{d}V$ spectra taken at the same area in linear scale. The tip heights refer to the set point of 1.7 V/0.8 nA (0 nm). The spectrum taken at 0.028 nm and 0 nm were offset by 12 pA/V and 27 pA/V for clarity, respectively. The green arrows indicate the peak position of defect states (E_d). (d) The energy of defect states (E_d) as a function of tip-sample distance.

Such energetic shifts of band edge and defect states might be caused by the tip-induced band bending (TIBB).[20] In low-conductivity semiconductors, the potential between tip and sample drops over not only the vacuum gap but also an extended region in the semiconductor, which gives rise to TIBB. As a result, the $\mathrm{d}I/\mathrm{d}V$ spectra may exhibit a considerable variation of the apparent bandgap. However, based on TIBB, the bandgap should appear substantially larger at smaller tip heights, which is contrary to our experimental results above. In addition, in our experiment, the E_F is very close to E_{CB}, which means that the sample is highly n-doped due to the high concentration of surface and subsurface defects. The high doping level of the sample may lead to efficient screening and thus negligible band bending.[30] Therefore, we can exclude TIBB as the origin of the energy shift.

The most possible origin of the bandgap narrowing is the image charge effect. When a point charge is placed before a metal tip, it induces a polarized cloud of opposite charges in the tip, which in turn lowers the energy of the point charge (Fig. 4(a)). In fact, the image charge effect can significantly renormalize the bandgap of semiconductor or molecular systems, leading to prominent band edge shift towards E_F.[23,25] The mechanism is schematically summarized in Fig. 4(b).

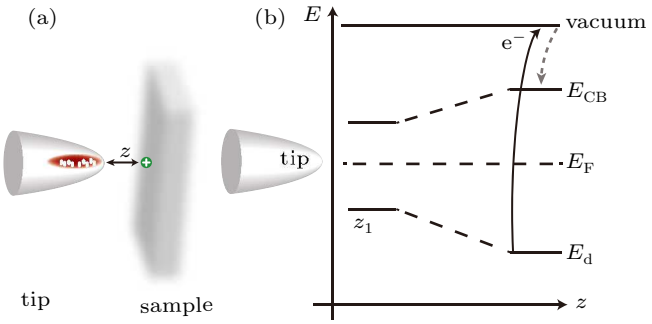


Fig. 4. (color online) (a) A positive charge (green) in the sample at a distance z from a metal tip can induce negative image charge (red) in the tip. (b) Schematic of band edge shift in TiO_2 as the metal tip approaches the surface arising from the image charge effect. The dash/solid arrow indicates an electron injected into/extracted from the conduction band/defect states of TiO_2.

When an electron is injected into the conduction band of TiO_2, the induced positive image charge in the tip will lower the electron energy, leading to the downward shift of the conduction band edge (E_{CB}). When the electron tunnels from the defect state to the tip, the hole created in the defect state also feels an attractive interaction from the negative image charge in the tip, which pushes up the defect state (E_d) towards E_F. Such a picture nicely explains the observed experimental results of light emission and $\mathrm{d}I/\mathrm{d}V$ measurements.

4. Conclusion and perspectives

We have investigated the plasmon-enhanced light emission of rutile TiO_2(110) surface by a low-temperature STM. The photon emission arises from the irradiative decay of LSP excited by the inelastic electronic transition between the STM tip and the conduction band or defect states of TiO_2(110). In contrast to the Au(111) surface, the maximum photon energy is not linear with the sample bias voltage, suggesting that the band edges are shifted towards the E_F when the tip height decreases. By performing differential conductance (dI/dV) measurements, we exclude the tip-induced band bending as the origin of band edge shifts. Instead, we propose that such band shifts arise from the image charge effect of the metal tip. This work not only sheds new lights onto the understanding of plasmon-enhanced light emission of semiconductor surfaces, but also opens up a new avenue for engineering the plasmon-mediated interfacial charge transfer in molecular and semiconducting materials.

References

[1] Gimzewski J K, Sass J K, Schlitter R R and Schott J 1989 *Europhys. Lett.* **8** 435
[2] Downes A and Well and M E 1998 *Phys. Rev. Lett.* **81** 1857
[3] Aizpurua J, Apell S P and Berndt R 2000 *Phys. Rev. B* **62** 2065
[4] Qiu X H, Nazin G V and Ho W 2003 *Science* **299** 542
[5] Dong Z C, Zhang X L, Gao H Y, Luo Y, Zhang C, Chen L G, Zhang R, Tao X, Zhang Y, Yang J L and Hou J G 2010 *Nat. Photon.* **4** 50
[6] Krane N, Lotze C, Lager J M, Reecht G and Franke K J 2016 *Nano Lett.* **16** 5163
[7] Berndt R, Gimzewski J K and Johansson P 1991 *Phys. Rev. Lett.* **67** 3796
[8] Suzuki Y, Minoda H and Yamamoto N 1999 *Surf. Sci.* **438** 297
[9] Dong Z C, Guo X L, Trifonov A S, Dorozhkin P S, Miki K, Kimura K, Yokoyama S and Mashiko S 2004 *Phys. Rev. Lett.* **92** 086801
[10] Wu S W, Nazin G V and Ho W 2008 *Phys. Rev. B* **77** 205430
[11] Cavar E, Blum M C, Pivetta M, Patthey F, Chergui M and Schneider W D 2005 *Phys. Rev. Lett.* **95** 196102
[12] Hoffmann G, Kliewer J and Berndt R 2001 *Phys. Rev. Lett.* **87** 176803
[13] Nazin G V, Qiu X H and Ho W 2003 *Phys. Rev. Lett.* **90** 216110
[14] Thirstrup C, Sakurai M, Stokbro K and Aono M 1999 *Phys. Rev. Lett.* **82** 1241
[15] Jackson J D 1975 *Classical Electrodynamics*, 2nd edn. (New York: John Wiley & Sons) p. 490
[16] Yim C M, Pang C L and Thornton G 2010 *Phys. Rev. Lett.* **104** 036806
[17] Zuo F, Wang L, Wu T, Zhang Z Y, Borchardt D and Feng P Y 2010 *J. Am. Chem. Soc.* **132** 11856
[18] Naldoni A, Allieta M, Santangelo S, Marelli M, Fabbri F, Cappelli S, Bianchi C L, Psaro R and Dal Santo V 2012 *J. Am. Chem. Soc.* **134** 7600
[19] Dombrowski R, Steinebach C, Wittneven C, Morgenstern M and Wiesendanger R 1999 *Phys. Rev. B* **59** 8043
[20] Berndt R and Gimzewski J K 1992 *Phys. Rev. B* **45** 14095
[21] Mcellistrem M, Haase G, Chen D and Hamers R J 1993 *Phys. Rev. Lett.* **70** 2471
[22] Kaasbjerg K and Flensberg K 2008 *Nano Lett.* **8** 3809
[23] Thygesen K S and Rubio A 2009 *Phys. Rev. Lett.* **102** 046802
[24] Barr J D, Stafford C A and Bergfield J P 2012 *Phys. Rev. B* **86** 115403
[25] Perrin M L, Verzijl C J O, Martin C A, Shaikh A J, Eelkema R, van Esch J H, van Ruitenbeek J M, Thijssen J M, van der Zant H S J and Dulic D 2013 *Nat. Nanotechnol.* **8** 282
[26] Cooper B R, Ehrenreich H and Philipp H R 1965 *Phys. Rev.* **138** A494
[27] Ehrenreich H and Philipp H R 1962 *Phys. Rev.* **128** 1622
[28] Minato T, Sainoo Y, Kim Y, Kato H S, Aika K, Kawai M, Zhao J, Petek H, Huang T, He W, Wang B, Wang Z, Zhao Y, Yang J L and Hou J G 2009 *J. Chem. Phys.* **130** 124502
[29] Wendt S, Sprunger P T, Lira E, Madsen G K H, Li Z S, Hansen J O, Matthiesen J, Blekinge-Rasmussen A, Laegsgaard E, Hammer B and Besenbacher F 2008 *Science* **320** 1755
[30] Zhang Z and Yates J T 2012 *Chem. Rev.* **112** 5520